5. Forshey, P. A.; Kuwana, T. *Inorg. Chem.* **1981**, *19*, 693.
6. Forshey, P. A.; Kuwana, T.; Kobayashi, N.; Osa, T. *Adv. Chem. Ser.* **1982**, *201*, 601.
7. Kuwana, T.; Fujihira, M.; Sunakawa, K.; Osa, T. *J. Electroanal. Chem.* **1978**, *88*, 299.
8. Ozer, D.; Harth, R.; Mor, U.; Bettelheim, A. *J. Electroanal. Chem.* **1989**, *266*, 109.
9. Ozer, D.; Parash, R.; Broitman, F.; Mor, V.; Bettelheim, A. *J. Chem. Soc., Faraday Trans. I* **1984**, *80*, 1139.
10. Bettelheim, A.; Parash, R.; Ozer, D. *J. Electrochem. Soc.* **1982**, *129*, 2247.
11. Bettelheim, A.; Ozer, D.; Parash, R. *J. Chem. Soc., Faraday Trans. I* **1983**, *79*, 1555.
12. Creager, S. E.; Raybuck, S. A.; Murray, R. W. *J. Am. Chem. Soc.* **1986**, *108*, 4225.
13. Creager, S. E.; Murray, R. W. *Inorg. Chem.* **1987**, *26*, 2612.
14. Perree-Fauvet, M.; Gandemer, A.; Bonvoison, J.; Girerd, J. J.; Boucly-Goester, C.; Boucly, P. *Inorg. Chem.* **1989**, *28*, 3533.
15. Tsang, P. K. S.; Sawyer, D. T. *Inorg. Chem.* **1990**, *29*, 2848.
16. Sazou, D.; Araullo-McAdams, C.; Han, B. C.; Franzen, M. M.; Kadish, K. M. *J. Am. Chem. Soc.* **1990**, *112*, 7879.
17. D'Souza, F.; Deviprasad, G. R.; Hsieh, Y.-Y. *J. Electroanal. Chem.* **1996**, *411*, 167.
18. Shigehara, K.; Anson, F. C. *J. Phys. Chem.* **1982**, *86*, 2776.
19. Ni, C. L.; Anson, F. C. *Inorg. Chem.* **1985**, *24*, 4754.
20. Durand, R. R.; Anson, F. C. *J. Electroanal. Chem.* **1982**, *134*, 273.
21. Shi, C.; Anson, F. C. *J. Am. Chem. Soc.* **1991**, *113*, 9564.
22. Shi, C.; Anson, F. C. *Inorg. Chem.* **1995**, *34*, 4554.
23. Steiger, B.; Anson, F. C. *Inorg. Chem.* **1994**, *33*, 5767.
24. Steiger, B.; Anson, F. C. *Inorg. Chem.* **1995**, *34*, 3355.
25. Collman, J. P.; Chang, L. L.; Tyvoll, D. A. *Inorg. Chem.* **1995**, *34*, 1311.
26. Collman, J. P.; Wagenknecht, P. S.; Hutchison, J. E. *Angew. Chem., Int. Ed. Engl.* **1994**, *33*, 1537.
27. Collman, J. P.; Denisevich, P.; Kanai, Y.; Marrocco, M.; Koval, C.; Anson, F. C. *J. Am. Chem. Soc.* **1980**, *102*, 6027.
28. Chang, C. K.; Liu, H. Y.; Abdalmuhdi, I. *J. Am. Chem. Soc.* **1984**, *106*, 2726.
29. Karaman, R.; Jeon, S.; Almarsson, O.; Blasko, A.; Bruice, T. C. *J. Am. Chem. Soc.* **1992**, *114*, 4899.
30. Jeon, S.; Almarsson, O.; Karaman, R.; Blasko, A.; Bruice, T. C. *Inorg. Chem.* **1993**, *32*, 2562.
31. Choi, Y-K.; Jeon, S.; Park, J-K.; Chjo, K-H. *Electrochim. Acta* **1997**, *42*, 1287.
32. Battersby, A. R.; Fookes, C. J. R.; Matcham, C. W. J.; McDonald, E. *Nature (London).* **1980**, *285*, 17.
33. Lin, X. Q.; B.-Cocolios, B.; Kadish, K. M. *Inorg. Chem.* **1986**, *25*, 3242.
34. Chan, R.; Su, Y. O.; Kuwana, T. *Inorg. Chem.* **1985**, *24*, 3777.

# Real Time Monitoring of Ionic Species Generated from Laser-Ablated $Pb(Zr_{0.52}Ti_{0.48})O_3$ Target Using Pulsed-Field Time-Of-Flight Mass Spectrometer

**Young-Ku Choi, Hoong-Sun Im†, and Kwang-Woo Jung***

*Department of Chemistry, Wonkwang University, Iksan 570-749, Korea*
*†Korea Research Institute of Standards and Science, Taeduk Science Town, Taejon 305-600, Korea*
*Received February 20, 1998*

The characteristics of the ablation plume generated by 532 nm Nd:YAG laser irradiation of a $Pb(Zr_{0.52}Ti_{0.48})O_3$ (PZT) target have been investigated using a pulsed-field time-of-flight mass spectrometer (TOFMS). The relative abundance of $O^+$, $Ti^+$, $Zr^+$, $Pb^+$, $TiO^+$, and $ZrO^+$ ions has been measured and discussed. $TiO^+$ and $ZrO^+$ ions were also found to be particularly stable within the laser ablation plasma with respect to $PbO^+$ species. The behavior of the temporal distributions of each ionic species was studied as a function of the delay time between the laser shot and the ion extraction pulse. The most probable velocity of each ablated ion is estimated to be $V_{mp}$=1.1-1.6$\times 10^5$ cm/s at a laser fluence of 1.2 J/cm$^2$, which is typically employed for the thin film deposition of PZT. The TOF distribution of $Ti^+$ and $Zr^+$ ions shows a trimodal distribution with one fast and two slow velocity components. The fast velocity component ($6.8\times 10^5$ cm/s) appears to consist of directly ablated species via nonthermal process. The second component, originated from the thermal evaporation process, has a characteristic velocity of 1.4-1.6$\times 10^5$ cm/s. The slowest component ($1.2\times 10^5$ cm/s) is composed of a dissociation product formed from the corresponding oxide ion.

## Introduction

Lead zirconate titanate, $Pb(Zr_xTi_{1-x})O_3$ (PZT), has attracted much attention due to the promise of applications in devices such as non-volatile random access memories,[1] electro-optic switches,[2] pyroelectric sensors,[3] and piezoelectric surface and bulk wave transducers.[4-6] Pulsed laser deposition (PLD) has become a powerful and efficient tech-

*Author to whom correspondence should be addressed.

nique for reproducibly depositing high-quality multicomponent thin films of PZT and other ceramics over the last few years.[7]

A most useful feature of PLD is that the stoichiometry of bulk target is preserved during the ablation and film deposition process, which in turn should result in better stoichiometric films. During the PLD process, a pulsed-laser beam of high energy density is used to ablate a solid target material. The various ablation products are predominantly ejected in the forward direction, normal to the target surface, and subsequently deposited on the substrate surface. Owing to its simplicity, PLD provides an excellent method of thin film fabrication for a vast variety of materials in a relatively short time.

Pulsed laser deposition of high quality PZT thin films was previously reported by our group.[8] In the course of the film optimization process, we observed various trends in variations of deposited film properties, some of which could not be fully explained. Many studies have also been reported on the fabrications of the PZT thin film, but the details of the ablation process have not been fully understood. For a given PLD system the resulting thin-film quality depends on such parameters as the laser energy density, the ambient oxygen pressure, and the target-to-substrate distance, all of which influence the chemical and physical properties of ejected material (plume). The main characteristics of PLD are closely connected to the plume composition and to the interaction of the ablated species with the gas environment. The analysis of the plume composition is very difficult due to several factors, such as the wide variety of ablated species, their high kinetic energy, and the complicated plasma reactions occurring inside the dense plume. Therefore, *in situ* monitoring of the ablation plume is desirable in order to control the growth quality of thin-film epitaxial oxides, and will likely be required in any eventual film manufacturing facility.[9]

Many diagnostics such as emission spectroscopy,[10] optical absorption spectroscopy,[11] laser-induced fluorescence spectroscopy,[12,13] time-integrated and time-resolved imaging,[14] and time-of-flight mass spectroscopy techniques[15] were applied to measuring ablation plasma parameters, to study flow dynamics of plume expansion and its subsequent interaction. Despite the many existing investigations on the ion emission of laser-produced plasmas, few experiments have been published on the ablation of a multielement solid target that could demonstrate directly the origin of the ejectant formation *i.e.*, electronic excitation, thermal process, chemical reactions, and dissociations during the plume propagation.

In this work, the pulsed-field TOFMS system has been used to observe the ionic species from laser-ablation of a PZT target and their dependence on laser energy density. The ablation process has been carried out under similar conditions to which PZT thin films were deposited.[8] Pulsed-field TOFMS during PLD makes use of the fact that a portion of the ablation products forms a highly forward-directed plume extending outward from the target surface. The relative abundance as well as the energy distribution of ejected ions among the ablation species are characterized by a time-delayed extraction of ions ablated off-axis to the flight direction.

## Experimental

The system consists of two main components: the laser ablation chamber and the mass spectrometer. Laser irradiation was provided by the second harmonic output (532 nm) of an Nd:YAG laser (Quanta-Ray; Model GCR-3) that produces pulses of 10 ns duration at a 10 Hz repetition rate. The laser beam strikes the surface of a PZT bulk target, at 45° to its surface normal, which is mounted on a rotatable target support. A plano-convex quartz lens with a 400 mm focal length created the spot of $3\times10^{-2}$ cm$^2$ on the target surface. The beam fluence at the target surface is 0.5 to 1.5 J/cm$^2$, which is typical energy density for the deposition of high-quality PZT films.[8] The laser ablation gives rise to the formation of a hot plume[16] consisting of electrons, ions, neutrals, and clusters. The detection of the ions present in the plume was performed using a pulsed-field time-of-flight mass spectrometer. Figure 1 shows a typical geometry for the laser ablation and time-resolved ion detection experiments. The ablated material evolves in the region between the repelling electrode and the collecting electrode with a 1.0 mm small hole to obtain a very narrow collection region.

As the plume reaches the TOFMS extraction region, the positive ions are extracted (following a delay of $\tau_d$=0-100 $\mu$s after the laser shot) by a +1500 V pulsed electric field, applied to the repelling electrode, and enter the orifice of the collecting electrode. The ions are then moved toward the microchannel plate (MCP) ion detector through the drift tube. This geometry places the ion flight path at right angles with the velocity vector of the ejected plume. The ion extraction pulse has a rise time of 40 ns and a duration of 4 $\mu$s. Since the ions in the ejected plume propagate in the field-free region of the source during the time $\tau_d$, the velocity components at directions normal to the ablation surface can be calculated from their delay times ($\tau_d$) and the distance between the target and extraction region.

In this study the target location relative to the center of the ion extraction region is fixed ($h$=0.4 inch) and the delay time is varied. For acceptable signal to noise ratios, all

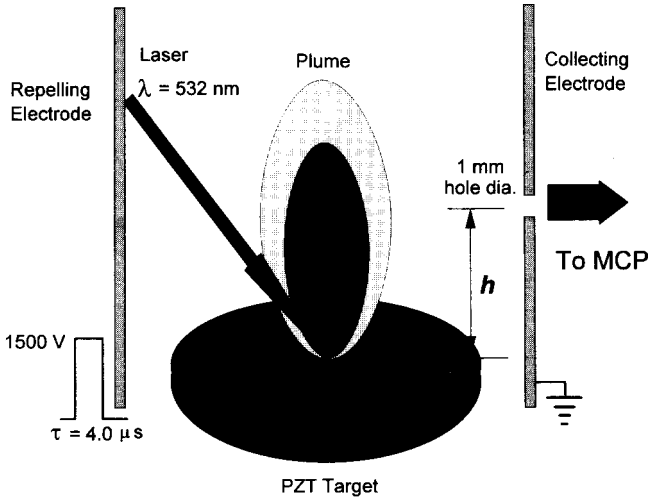


**Figure 1.** Typical geometry for the laser ablation and time-resolved ion detection experiments.

mass spectra in the present experiment were obtained by a cumulative collection of 300 laser shots. The whole vacuum system is pumped by a Turbomolecular pump. The background pressure at the laser ablation chamber is $5\times10^{-7}$ Torr. The bulk target obtained from Ssangyong Research Center consists of a single-phase pellet of $Pb(Zr_{0.52}Ti_{0.48})O_3$ with 2 wt.% of SrO.

## Results and Discussion

The effect of laser energy density (*i.e.*, the fluence) at the target surface was investigated over a range of 0.5-1.5 J/cm$^2$. At this fluence range, the vapour density directly above the target surface is generated in the first few nanoseconds of the laser pulse. Interaction of the remaining energy in the laser pulse with the vapourized material switches the ablation mode to a plasma-dominated regime.[17]

Figure 2 shows the typical TOF spectra obtained from laser ablation of a PZT target with a laser pulse energy of 0.5 J/cm$^2$ in high vacuum ($p\approx5\times10^{-7}$ Torr). As can be easily seen from this figure, the spectra mostly consist of the monatomic ions ($Ti^+$, $Zr^+$, and $Pb^+$) and the ionized oxides ($TiO^+$, $ZrO^+$, and $PbO^+$), whereas the heavy polyatomic molecular ions and clusters with masses higher than the diatomic oxides do not appear. The relative intensities of $Ti^+$, $Zr^+$, and $Pb^+$ ions are inconsistent with the normal composition of the $Pb(Zr_{0.52}Ti_{0.48})O_3$ bulk target. This feature is presumably due to the difference in ionization potential, vapor pressure, and oxide binding energy of these atoms in the laser-produced plume; 6.82 eV(Ti), 6.84 eV(Zr), and 7.42 eV(Pb).

The overall emission of ionic species lasts until 6 $\mu$s. The $Ti^+$ and $Zr^+$ ions show a broad temporal distribution, indicating that these ions are ablated with a wide range of velocity components. It is interesting to note that the temporal distribution of the $Pb^+$ ion is narrow in spite of the high volatility of Pb with respect to the other elements of the PZT target,[18] as will be discussed in more detail later.

Increasing the laser fluence, the spectra are characterized by the increase of atomic and oxide species abundance and the occurrence of $O^+$ and $PbTiO^+$ ions (see Figure 3). The result indicates, as expected, that as the laser fluence is increased, more material is ablated from the target and emits. The production of the monoxide ions $TiO^+$ and $ZrO^+$ as well as their monatomic ions is clearly observed, whereas Pb is predominantly present in the form of a monatomic ion. Recently, the dynamics of laser ablation of PZT have been studied by Tyrrell *et al.* using a quadrupole mass spectrometer.[19] They have isolated the characteristic elemental and molecular ionic $Ti^+$, $Zr^+$, $Pb^+$, $TiO^+$, $ZrO^+$, and $O^+$ species during the 532 nm irradiation of a PZT target at a laser fluence of 5 J/cm$^2$, which is in good agreement with our current observation. The temporal distribution of the ejected species shows quite a broad distribution as compared with the result at low laser fluence (see Figure 2). This observation implies that an increase in the irradiance results in a broad emission of ions which lasts ~13 $\mu$s.

The presence of oxide ions in the laser ablation plasma is a subject of great interest since these molecular ions are known to influence thin film growth of multicomponent oxides quite significantly. As a general trend in the present study, the abundances of monoxide ions are always lower than their corresponding atomic ions; this behavior can be ascribed to the fact that the monoxide ions take part in the formation of atomic ions in the early stage of laser ablation, thus their relative abundance results lowered. The $ZrO^+$ ions are found to be particularly stable within the laser ablation plasma with respect to $TiO^+$ and $PbO^+$ species. The dissociation energy of the molecular ion appears to be a crit-

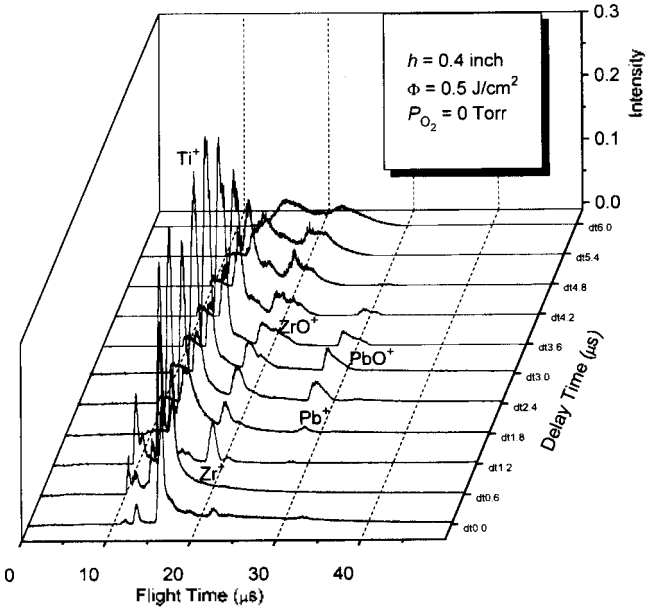


**Figure 2.** TOF spectra of laser ablated ions from a PZT target in high vacuum as a function of delay time between the laser shot and the extraction pulse: target to extraction zone distance $h$= 0.4 inch. The ions were ablated by 532 nm with a pulse energy of 0.5 J/cm$^2$.

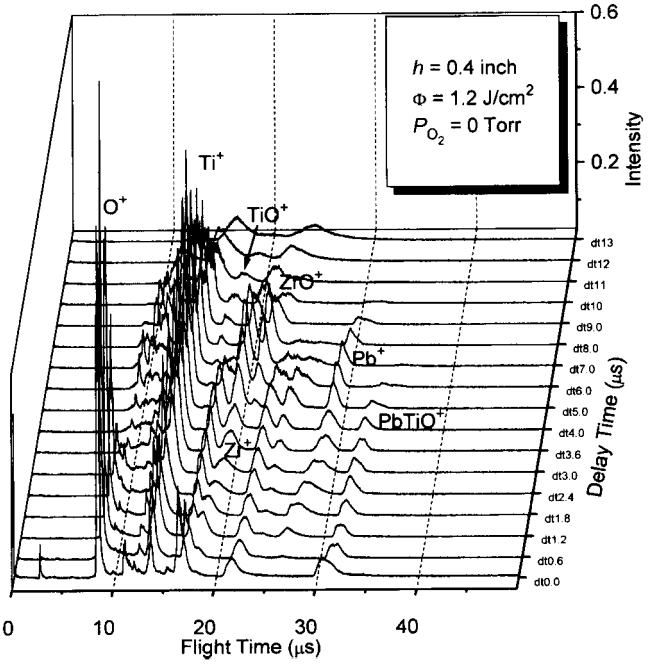


**Figure 3.** TOF spectra obtained from laser ablation of a PZT target with a laser pulse energy of 1.2 J/cm$^2$ in high vacuum.

ical indicator of its stability in the laser produced plasma. The bond dissociation energies, $D_o$, of the diatomic species are 6.8, 8.0, and 2.2 eV respectively for $TiO^+$, $ZrO^+$, and $PbO^+$.[20] The weak bond dissociation energy of the $PbO^+$ ion is suggestive of the fact that the $PbO^+$ ion would presumably have a greater opportunity to dissociate into $Pb^+$+O during the ablation. The early ejection of the polyatomic $PbTiO^+$ ion is quite interesting. Such an occurrence indicates that $PbTiO^+$ is produced by direct evaporation from the target, rather than by a reaction between ablated Pb, Ti, and O atoms during the plume propagation. It is considered that this type of ablation is initiated by the photochemical fragmentation.

In the present experiment, the time-of-flight measurement of the ablated ions was triggered by the laser irradiation. Thus, the increase of delay time between the laser shot and ion extraction pulse indicates the increased flight time of the collected ions through the axis perpendicular to the TOFMS detection axis. The increase corresponds to the greater time necessary to travel from the target to the collection region of the mass spectrometer. Therefore, one of the great strengths of a pulsed-field TOFMS study is that by varying the delay time the temporal profile of each ion can be obtained, permitting accurate measurement of the velocity distribution as well as drift velocity of the ionic species.

The intensities of the ablated ions were plotted as a function of the delay time of the ion extraction pulse as shown in Figure 4. The intensities of the $O^+$ and $Ti^+$ ions were multiplied by 1/6 and 1/3, respectively, for display purposes. A narrow temporal distribution of the $O^+$ ion is ascribed to the nonthermal (electronic) process, i.e., direct photochemical interaction, where rapid energy deposition gives rise to electronic transitions of the chemical bonds in solid surface to antibonding states resulting in the production of photofragments with a fast and narrow velocity distribution, and subsequent ionization within the relatively high-density plume.[21]

The figure shows also that in general heavier species go through local maxima with a longer delay time. It is known that the velocity and acceleration of the species in the plasma depend on the molecular weight of the respective species. Since the plasma from the PZT surface is composed of atoms and molecules of different atomic weights (O=16.0, Ti=47.9, Zr=91.2, and Pb=207.2), the expansion velocity of each of the species would not be the same. Singh and Narayan[22] proposed an adiabatic expansion model in which a high-temperature, high-pressure laser-heated plasma is formed directly above the surface. The model predicts an inverse square-root dependence of the atomic asymptotic velocities with mass. The observed discrepancy for $TiO^+$ and $Pb^+$ ions in the present measurements is probably due to the interaction (mixing effect) of different atomic species present in the plume.

The most probable velocities can be estimated from the delay time showing maximum intensities and the target location relative to the center of the ion extraction region (or TOFMS detection axis). The most probable velocities for $Ti^+$, $Zr^+$, $TiO^+$, $ZrO^+$, and $Pb^+$ ions lie in the range of $V_{mp}$= 1.1-1.6$\times 10^5$ cm/s. In addition, two velocity components can be distinguished in the case of $Ti^+$ and $Zr^+$ ions, suggesting two different ejection mechanisms. The narrow and small peak with nearly the same maximum at 1.5 $\mu$s may be attributed to a nonthermal distribution ($V_{mp}$ 6.8$\times 10^5$ cm/s), while the second and broad peaks with maxima at 6.3 $\mu$s ($Ti^+$) and 7.5 $\mu$s ($Zr^+$) correspond to a Maxwellian distribution of thermally evaporated $Ti^+$ and $Zr^+$ ions. The similar peak velocity of fast component with that of $O^+$ ion also supports our conclusion that the fast component is originated from the direct nonthermal ejection mechanism. The slow velocity component, however, has the lower energy spreads characteristic of thermally produced ions and is probably observed whenever the substrate is unable to dissipate the laser energy promptly.

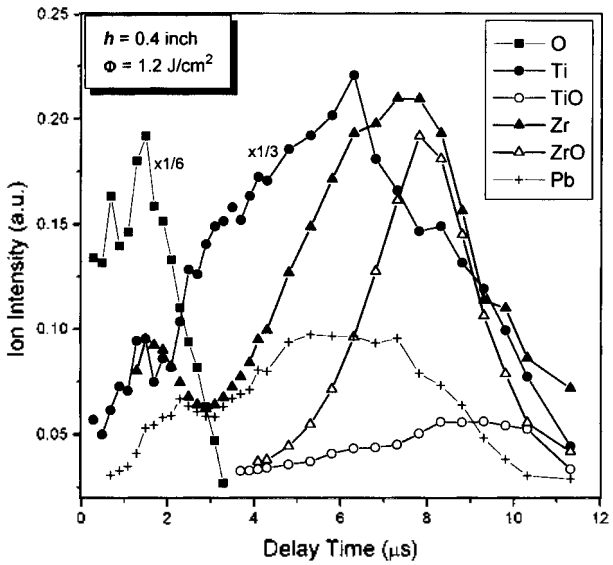


**Figure 4.** The ion intensities of the ablated species as a function of delay time between the laser irradiation and the extraction pulse at $h$=0.4 inch following 1.2 J/cm$^2$ laser irradiation of a PZT target. The $O^+$ and $Ti^+$ ions data was scaled by 1/6 and 1/3, respectively, to facilitate comparison.

The narrow temporal distribution of $ZrO^+$ ion indicates that most or all of the $ZrO^+$ signal is from ZrO neutrals, with negligible contributions from the decomposition of large cluster. Alternatively, the $ZrO^+$ ions can be created by plasma reactions in the plume. If $ZrO^+$ ions are expected to be created by the collision between the high energy $O^+$ ions and Zr atoms, they should have high drift velocity. The observation of the slow velocity component of $ZrO^+$ ions also demonstrates that these ions derive directly from the target surface *via* thermal evaporation rather than being created by reactive or collisional processes within the plasma. On the other hand, the measured temporal distributions of the $Ti^+$ and $Zr^+$ ions show a much broader distribution compared with those of the $TiO^+$ and $ZrO^+$ ions. It is implied by such a wide energy distribution that the ablation mechanism generating these species is very complicated.

In order to understand more fully the origin of the fast and slow velocity components we investigated the temporal distribution of $Ti^+$ ions as a function of laser fluence. Figure 5 displays a plot of $Ti^+$ ion intensities as a function of delay time at three different laser fluences. Clearly two features are obvious in the figure, one a weak, "fast" velocity component and the other a "slow" velocity component. The fast

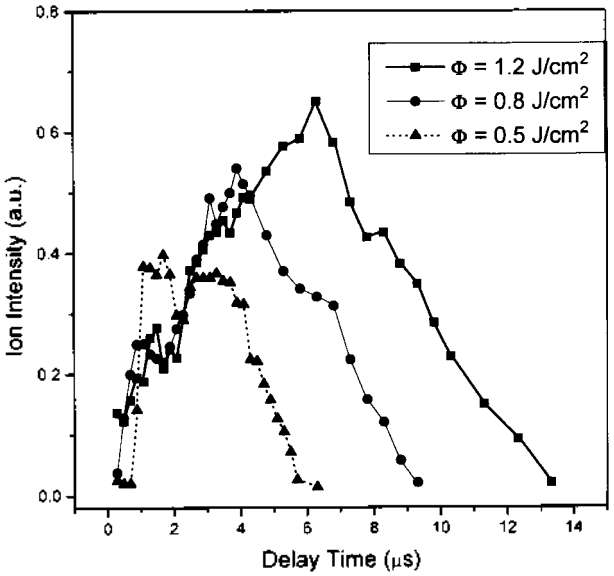


**Figure 5.** Plot of the $Ti^+$ ion intensities as a function of delay time at three different laser fluences.

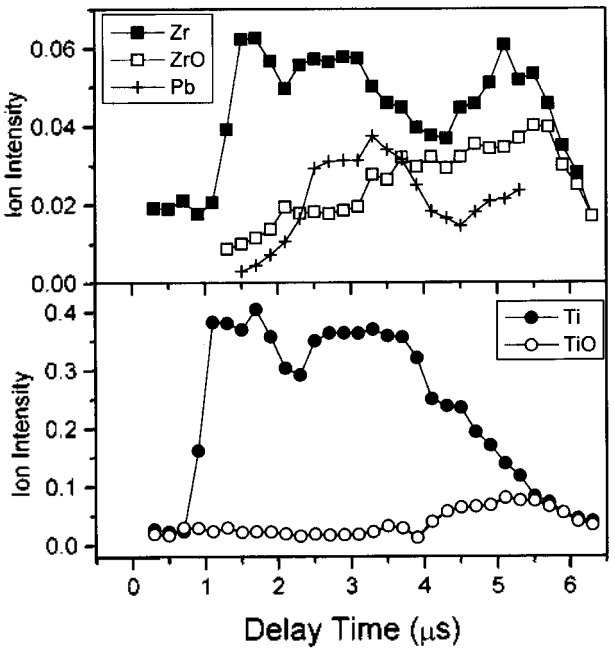


**Figure 6.** Comparisons of monatomic and monoxide ion intensities as a function of delay time at 0.5 J/cm² laser fluence.

component exhibits a very nonthermal distribution (having a high velocity peak and a narrow distribution), which is insensitive to the fluence range of $\Phi$=0.5-1.2 J/cm². The incident laser energy, on one hand, is used to break the chemical bonds in solid surface and on the other hand, is converted into kinetic energy of the ablated species. Whatever the fluence is, the photon energy needed to break the chemical bonds is the same. For this reason, the fast component results from the direct ejection in the atomic form *via* nonthermal process followed by the multiphoton or free-electron impact ionization within the expanding plasma.

The most probable velocity and its distribution of the slow component is greatly influenced by the laser fluence. As the fluence is increased, the peak of the slow velocity component moves toward longer time-of-flight and keeps on broadening, but its magnitude, in contrast to that of the fast peak, continuously grows. A similar trend has also been found in XeCl laser ablation of a PZT target,[23] in which the thermal evaporation component increases and becomes more important at high fluence. Based on the above results, we believe that the thermal process in the laser ablation plays an important role as increasing the laser fluence.

The broadening of the slow velocity component at high laser fluence can be explained by the increased plume temperature as well as the scattering mechanism over extended distances in which ions and atoms in the ablation plume undergo collisions, thus distorting the nascent mass and velocity distributions. The plume material is retarded from the fast vacuum velocity distribution due to momentum transfer with the background gas (as well as other retarded plume material). For this reason, one can attribute the decrease in most probable velocity of a slow component with laser fluence to the gas collision between the plume ejectants in the high pressure region of the initial expansion, resulting in a Knudsen layer with stopped and/or backward moving material.[24,25]

Another distinct feature to be noted is that, as shown in Figure 5, a third component of the plume appears on the falling edge of the slow component, *i.e.*, 4.3 μs ($\Phi$=0.5 J/cm²), 6.8 μs ($\Phi$=0.8 J/cm²), and 8.3 μs ($\Phi$=1.2 J/cm²). In order to determine the origin of these much later arriving materials, we plotted the ion intensities as a function of delay time at $h$=0.4 inch following 0.5 J/cm² laser irradiation. Figure 6 shows that the temporal distributions of $Ti^+$ and $Zr^+$ ions distinctly split into three peaks, one fast and two slow ones. The slow velocity components of $Zr^+$ and $Ti^+$ ions can be explained by the two different mechanisms. Either Ti (and Zr) atom is ablated intact *via* thermal evaporation process and subsequently excited to form a $Ti^+$ (and $Zr^+$) ion by free electrons in the expanding plasma, or a $Ti^+$ (and $Zr^+$) ion is formed through the dissociation reaction of oxide ions, $MO^+ \rightarrow M^+ + O$, where M denotes the Ti and Zr atoms. It has been known that the laser ablation of Pb is dominated by thermal evaporation even at the intermediate laser fluences, as Pb and its corresponding oxides have relatively low melting temperatures. The slow components of $Ti^+$ (2.7 μs) and $Zr^+$ (3.0 μs) ions show a similar drift velocity and distribution with that of a $Pb^+$ ion, indicating that these components arise from the thermal process.

The slowest velocity component of $Ti^+$ and $Zr^+$ ions is not a direct ablation product, but rather is formed within the plume by a secondary process, *i.e.*, dissociation of $TiO^+$ and $ZrO^+$ ions. It is conceivable that the highly excited oxide ions heavier than the monatomic ions may spontaneously fragment into lighter ions since they are reasonably supposed to have enough internal energy. In such a case, the bond breaking and/or energy release by translation of the fragments should effectively play a role as a major cooling process for the hot particles. The similarity in the slowest velocity distributions of $Ti^+$ and $Zr^+$ ions with those observed for the $TiO^+$ and $ZrO^+$ strongly suggests the dissociation of oxide ions during the plume propagation. There are two likely mechanisms for the dissociation of these monoxide ions. The first is the photodissociation by ab-

sorbed laser energy which could proceed *via* a multiphoton absorption process. Secondly, collisional phenomena within the plasma could account for the dissociation.

In the light of these observations, one concludes that three types of $Ti^+$ and $Zr^+$ ions are considered in the laser-ablated plume: (i) nascent atomic ions that are ejected from the target by electronic excitation, (ii) thermally evaporated atomic ions, and (iii) those from the dissociation of the diatomic or polyatomic species ejected from the target.

## Conclusion

The pulsed-field TOFMS technique was used to characterize the evolution of charged species in the laser ablation of a PZT target. The analysis of mass spectra has been carried out as a function of delay time between the laser shot and the ion extraction pulse. The dominant ions in the mass spectra consist of monatomic $Ti^+$, $Zr^+$, and $Pb^+$ species, whereas the monoxide ions, such as $TiO^+$, $ZrO^+$, and $PbO^+$, show only small contributions. Time-resolved analysis of the temporal evolution of the ionic species shows that the emission spreads over some tens of microseconds. As the laser fluence is increased, the overall ion intensiy increases and its distribution becomes broad due to the dominant contribution from the thermal evaporation process. The temporal distribution of $Ti^+$ and $Zr^+$ ions consists of three components, one from nonthermal process, another from thermal evaporation, and the other from dissociation of oxide ions. Because the present experiments monitor the plume itself, the instrument has the advantages of direct monitoring of the laser-ablated material that is in the process of becoming a thin film, thereby providing an important *in situ* diagnostic for pulsed laser deposition. A detailed description of the plume propagation and implications for plume temperatures will be presented elsewhere.

**Acknowledgment.** This work was supported by Wonkwang University in 1997.

## References

1. Myers, E. R.; Kingon, A.; Tuttle, B. in *Proc. Mater. Res. Soc.*, Spring Meeting Symp. on Ferroelectric Thin Film II (Materials Research Society, Pittsburgh, PA, 1991).
2. Adachi, G.; Mitsuyu, T.; Yamazaki, O.; Was, K. *J. Appl. Phys.* **1986**, *60*, 763.
3. Ichinose, N.; Hirao, Y.; Nakamoto, N.; Yamashida, T. *Jpn. J. Appl. Phys.* **1985**, *24*, 463.
4. Krupanidhi, S. B.; Sayer, M.; El-Assal, K.; Jen, C. K.; Farnell, G. W. *J. Can. Ceram. Soc.* **1984**, *54*, 28.
5. Okuyama, M.; Hamakawa, Y. *Ferroelectrics* **1985**, *63*, 243.
6. Sreenivas, K.; Sayer, M.; Barr, D. J.; Nishioka, M. *Appl. Phys. Lett.* **1988**, *52*, 709.
7. Chrisey, D. B.; Hubler, G. K. *Pulsed Laser Deposition of Thin Films*; Wiley: New York, 1994.
8. Im, H.-S.; Kim, S.-H.; Choi, Y.-K.; Lee, K. H.; Jung, K.-W. *Bull. Korean Chem. Soc.* **1997**, *18*, 56.
9. Li, Q.; Liu, S.; Fenner, D. B.; Luo, J.; Hamblen, W. D.; Haigis, J. *IEEE Trans. Appl. Supercond.* **1995**, *5*, 1513.
10. Geohegan, D. B. *Appl. Phys. Lett.* **1992**, *60*, 2732.
11. Geohegan, D. B. *Laser Ablation: Mechanisms and Applications*; Springer: Heidelberg, 1991; p 28.
12. Otis, C. E.; Dreyfus, R. W. *Phys. Rev. Lett.* **1991**, *67*, 2102.
13. Otis, C. E.; Goodwin, P. M. *J. Appl. Phys.* **1993**, *73*, 1957.
14. Geohegan, D. B.; Puretzky, A. A. *Appl. Phys. Lett.* **1995**, *67*, 197.
15. Hansen, S. G. *J. Appl. Phys.* **1989**, *66*, 3329.
16. Ready, J. F. *J. Appl. Phys.* **1965**, *36*, 462.
17. Vertes, A.; Gijbels, R.; Adams, F. *Anal. Chem. Anal. Ser.*; Wiley: New York, 1993; Vol. 124.
18. Horwitz, J. S.; Grabowski, K. S.; Chrisey, D. B.; Leuchtner, R. E. *Appl. Phys. Lett.* **1991**, *59*, 1565.
19. Tyrrell, G. C.; York, T. H.; Coccia, L. G.; Boyd, I. W. *Appl. Surf. Sci.* **1996**, *96*, 769.
20. Radzig, A. A.; Smirnov, B. M. *Reference Data on Aoms, Molecules, and Ions*; Springer-Verlag: Berlin, Germany, 1985.
21. Miller, J. C. *Laser Ablation: Principles and Applications*; Springer-Verlag: Berlin, Germany, 1994.
22. Singh, R.; Narayan, *J. Phys. Rev. B* **1990**, *41*, 8843.
23. Hau, S. K.; Wong, K. H.; Chan, P. W.; Choy, C. L.; Wong, H. K. *J. Mater. Sci. Lett.* **1992**, *11*, 1266.
24. Kelly, R.; Braren, B. *Appl. Phys. B* **1991**, *53*, 160.
25. Kelly, R. *J. Chem. Phys.* **1990**, *92*, 5047.